Light Metals 2011 *Edited by: Stephen J. Lindsay*
TMS (The Minerals, Metals & Materials Society), 2011

STUDY OF ELECTROMAGNETIC FIELD IN 300KA ALUMINUM REDUCTION CELLS WITH INNOVATION CATHODE STRUCTURE

Baokuan Li[1],Xiaobo Zhang[1], Sui-rui Zhang[1], Fang Wang[1], Nai-xiang Feng[1]

[1] School of Materials & Metallurgy, Northeastern University, Shenyang 110819, China
[2] School of Materials & Metallurgy, Wuhan University of Science and Technology, Hubei 430081, China

Keywords: aluminum reduction cells; innovation cathode structure; electromagnetic field; numerical simulation

Abstract

Three dimensional steady finite element models have been developed to study the effect of the novel structure cathode (NSC) on the electromagnetic field in aluminum reduction cells. In addition to reduction cells, the finite element system includes the busbar, ferromagnetic shell and air. Numerical results show the current density, magnetic flux density, electric potential and electromagnetic force is different between NSC and traditional cells. The NSC with the convex block can divide the aluminum melt into a number of parts, where the electromagnetic force decreases. There are different small circulations formed around the convex blocks in aluminum melt, which not only reduce the fluctuation and the anode effect caused by lower alumina concentration, but also promote the dissolution of alumina. Compared to the traditional aluminum reduction cells, the NSC cells have the advantage of reasonable current density distribution and relatively uniform electromagnetic force distribution, so that the aluminum melt has smaller fluctuations and higher efficiency of current.

Introduction

Aluminum production consumes large amounts of energy, requiring 14000 ~ 14500kWh/T-AL for 1t[1]. On the other hand, the current efficiency and thus energy efficiency in the aluminum reduction cell may be decreased due to the melt accelerating cyclic aluminum surface uplift, deflection and fluctuation[2-3]. The Novel Structural Cathode (NSC)[7] technology, shown in Fig. 1, has a pattern of raised ridges where the flow field of molten aluminum shall be divided[4]. The ridges decrease the flow velocity and weaken significantly the effect of electromagnetic force and gravity waves of molten aluminum. Coupled action of electric field, magnetic field, flow field and joule-heat field in aluminum reduction cells has a significant influence on the current efficiency, energy consumption and the cells life[5-6]. So, deeper understanding of the coupled relation of electric field, magnetic field-three field, choosing the appropriate mathematical model, and improving precision of computed results are very important in theoretic and practical guideline for improving of the optimization, design, engineering analysis and development of new cells[7].

In this paper, the model of the structure of NSC systems is set up using PRO/E. Based on ANSYS platform, the finite element models of traditional and NSC cells are established to simulate the electromagnetic coupling field, using the equivalent resistance network method and edge element method.

Equations

The Maxwell equation, Lorentz law and Joule law describing the magnetic field is:

Ampere law: $$\nabla \times \vec{H} = \vec{J} + \frac{\partial \vec{D}}{\partial t} \quad (1)$$

Faraday law: $$\nabla \times \vec{E} = -\frac{\partial \vec{B}}{\partial t} \quad (2)$$

Gauss law: $$\nabla \cdot \vec{D} = \rho \quad (3)$$

Constitutive equation of magnetic flux is $\nabla \cdot \vec{B} = 0$ (4)

Since the frequency is less than 50Hz, the displacement current is ignored, as $\frac{\partial \vec{D}}{\partial t} = 0$.

As follows from Equation (2), the electric field is irrotational, and can be derived from:

$$\vec{E} = -\nabla V \quad (5)$$

electric scalar potential equation for electrostatic analysis is derived from governing Equation (2) and Equation (4), and constitutive Equation (3):

$$-\nabla(\vec{\varepsilon}(\nabla V)) = \rho \quad (6)$$

Equation (6) is solved in an electrostatic field analysis of dielectrics with the conductor of anode, electrolyte, molten aluminum and the cathode using elements SOLID231.

The equivalent resistance network model is used to solve the busbar system, according to Kirchhoff's law. The current distribution is calculated by Equation (7) to solve the potential of each node and the current of the busbar segment by choosing SOURC36 unit. :

$$\sum V_j = 0 \quad \sum I_j = 0 \quad (7)$$

Where $\vec{J} = \sigma(\vec{E} + \vec{v} \times \vec{B})$, (8)

$$\vec{B} = \nabla \times \vec{A}, \quad \vec{E} = -\frac{\partial \vec{A}}{\partial t} - \nabla \vec{V} \quad (9)$$

Lorentz law: $$\vec{F} = \vec{J} \times \vec{B} \quad (10)$$

where $\vec{H}$ is Associated magnetic flux density; $\vec{J}$ is total current density vector; $\vec{D}$ is electric flux density vector; $\vec{F}$ is Lorentz force; $\vec{B}$ is magnetic flux density vector; $\vec{E}$ is electric field intensity vector; $\vec{A}$ is magnetic vector potential; $\vec{V}$ is magnetic vector potential; Q is Joule heating; ρ electric charge density; σ is electrical conductivity matrix; ε is permittivity matrix; μ is magnetic permeability; $\vec{v}$ is velocity vector; V is electric scalar potential; $\vec{\omega}$ is joule-heat power density; t is time.

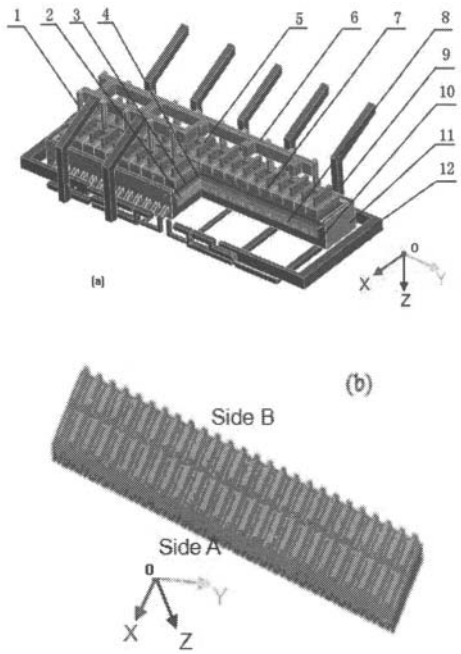

1. Aluminum conduction rod 2. Cathode 3. Cryolite 4. Aluminum melt 5. Anode rod 6. Anode bus bar 7. Anode 8. Cathode collector bar 9. Riser bus bar 10. Ramming paste 11. Steel shell 12. Cathode bus bar

Fig.1 Structure of 300kA cell with NSC technology

Method and gridding

The commercial package ANSYS 10.0, which is based on the finite element method, is used to analyze the electromagnetic field and the current field system. Nodal-based method (Solid117 element type) is used to solve the three–dimensional static electromagnetic field. The current amplitude loaded on the upper surface of the anode rod is 300KA with coupled VOLT freedom, and the electric potential on the top surface of the cathode collector bar is zero. The relative permeability of the electric conductor is set to 1. The physical properties, geometrical and operating conditions are shown in Tables 1 and 2. Fig 1 shows a schematic of the cell that was modeled.

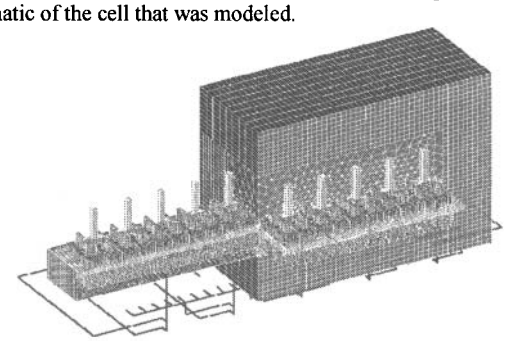

Fig.2 The finite element mesh model of electromagnetic field with a quarter of the air

The mesh system is shown in Figure 2, where the cathode and metal pad are meshed by structural grid and electrolyte and air are meshed by nonstructural grid. The total number of finite elements is 245542.

Table1 Geometry and operating parameters of the aluminum reduction cell

Geometry /m		Parameter	
Chamber	14.85×4.20×1.34	Current /KA	300
Anode carbon	1.64×0.66×0.55	Voltage /V	4
Cathode	3.44×0.51×0.45	Number of bar	26
Cathode Bus	1.57×0.18×0.13	Number of bus	26

Table 2 Physical parameters for electromagnetic field calculation

Parameters of electrical($\Omega \cdot m$)	
Resistance of molten aluminum	2.4×10^{-7}
Resistance of electrolyte	4.5×10^{-3}
Resistance of carbon anode	3.5×10^{-5}
Resistance of steel yokes	2.34×10^{-7}
Resistance of cathodes	3.8×10^{-5}
Resistance of the cathode bar	7.78×10^{-7}

Result and discussion

The current density distribution

The total current density distributions of (a) traditional aluminum cell (b) NSC cell are shown in Figure 3.The current density distribution of the traditional cell is more uniform than that of the NSC cell, due to the flatness of the traditional cell compared to the projections from the surface of the NSC cell.

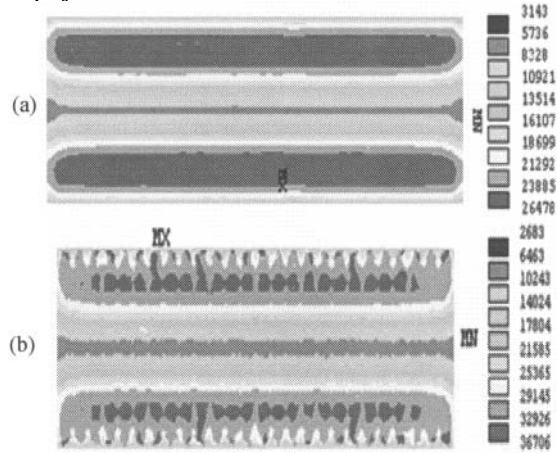

Fig. 3 The total current distribution on the bottom surface of molten aluminum

(a) Traditional cell (b) NSC cell

Figure 4 is a cross sectional view of the current densities (x direction on figure 1). Both distributions are symmetrical about the centerline of the cell, but the traditional cell has a more uniform distribution with lower maximum values.

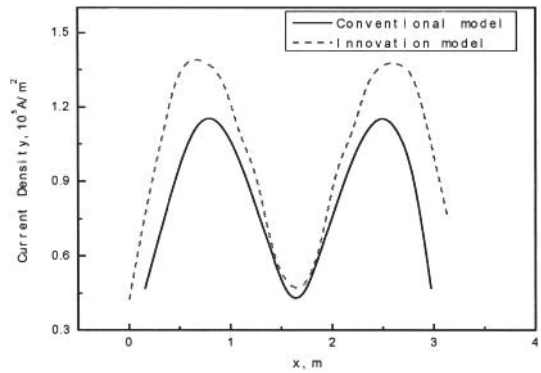

Fig. 4 The current density distribution on the cross section of molten aluminum in the traditional and NSC cell

The potential distribution

The potential distributions of molten aluminum for the two types of cathode are shown in Figures 5 and 6. The potential distributions are symmetrical along both the long and short axes. The maximums are at the short ends; the minimums are at the long sides. The voltage drop of the traditional cell is 0.009V; compared to 0.006V for the new cell from table 3.

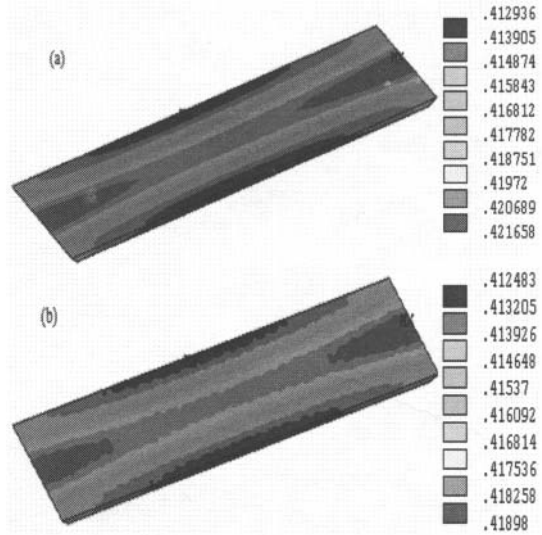

Fig.5 The molten aluminum potential distribution (a) tradition aluminum cell (b) innovation aluminum cell

The potential distribution of aluminum rod, steel yoke and anode block is the same in the new and traditional cathodes, as their structure, materials, and electrical load are the same. In both cells the anode assembly voltage drop is 0.638V from the top of the rod to the bottom of the anode block.

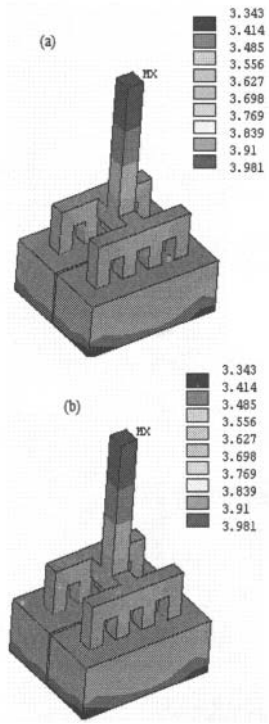

Fig.6 The anode system unit potential distribution (a) Traditional cell (b) NSC cell

The voltage drops in the two cells are shown in Table 3. The total voltage drop of the NSC cell is 0.066V lower than the traditional one, so the new cathode is more energy-efficient. A little more than half of the gain comes from the 0.035V difference in the electrolyte.

Table 3 voltage drop of traditional and NSC cell

parameter	tradition aluminum cell	innovation aluminum cell
voltage drop of cathode	0.248	0.219
voltage drop of anode	0.638	0.638
voltage drop of electrolyte	2.959	2.924
voltage drop of molten aluminum	0.009	0.006
voltage drop of cathode bar	0.336	0.337

The magnetic flux density distribution

The magnetic flux density B_x, B_y and B_z distribution of molten aluminum in the two types of cell is shown in Figures 7-10. Both cathode structures show the same type of symmetry: B_x and B_z have inverse symmetry along the short axis while B_y has symmetry along the long axis as well as the inverse symmetry along the short axis. The fluctuation of molten aluminum in the traditional cell is more intense. Magnetic induction B_x, B_y have little difference in value, while the magnetic induction B_z has slightly larger difference in value. That means the molten

aluminum is predicted to have better flow stability in the new cathode.

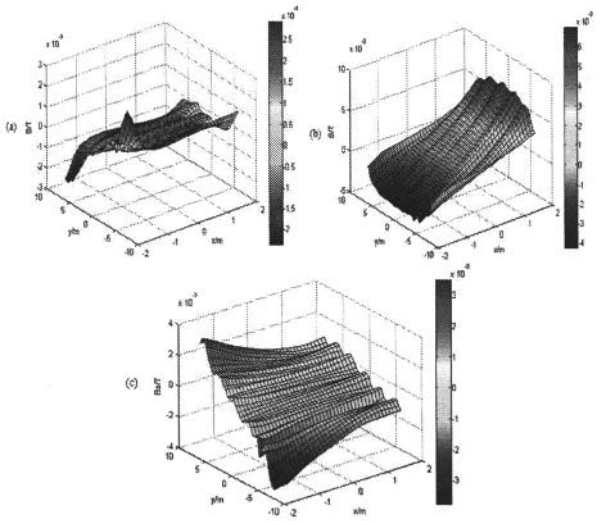

Fig. 7 The magnetic density distribution of molten aluminum in the traditional cell

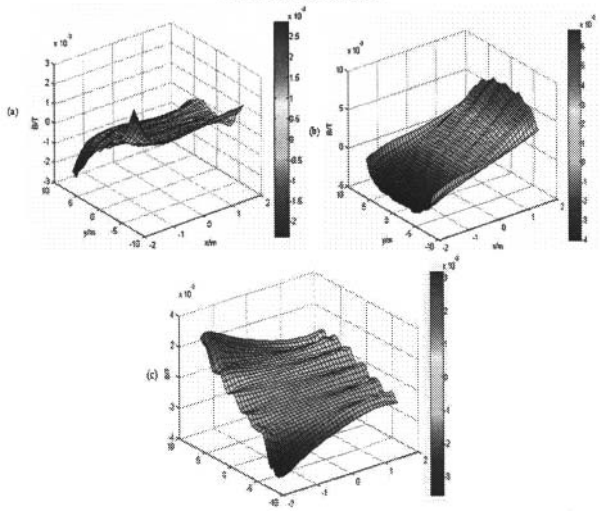

Fig. 8The magnetic density distribution of molten aluminum in the NSC cell

Table 4 Magnetic density on different plane of molten aluminum in the NSC cell

parameter	Top of molten aluminum	Bottom of molten aluminum
$\|B_x\|_{max}$	31.23	23.79
$\|B_x\|_{ave}$	4.13	3.87
$\|B_y\|_{max}$	70.82	62.65
$\|B_y\|_{ave}$	24.11	22.18
$\|B_z\|_{max}$	37.77	30.24
$\|B_z\|_{ave}$	8.86	7.83
$\|B\|_{max}$	70.82	62.65
$\|B\|_{ave}$	28.19	25.68

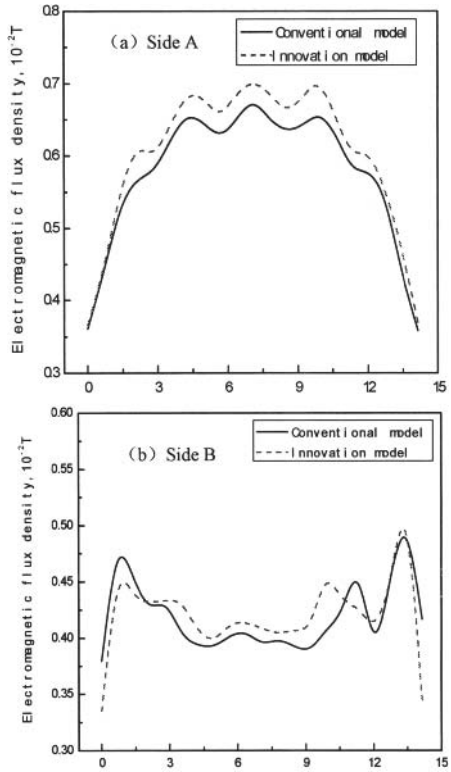

Fig. 9 The magnetic density distribution of molten aluminum

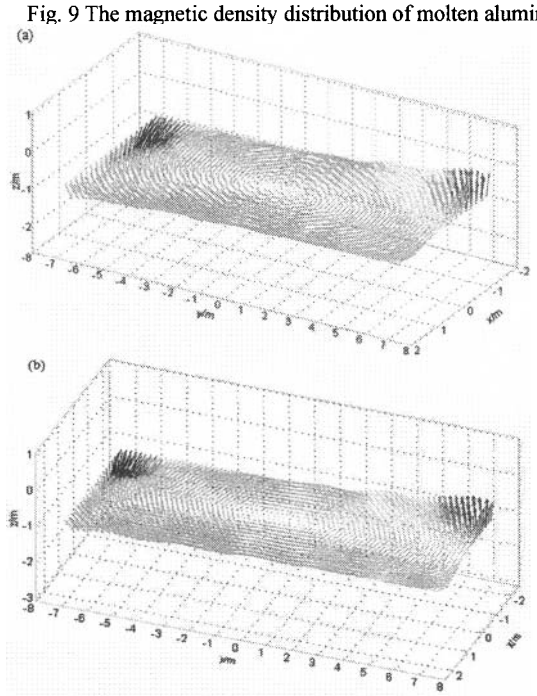

Fig. 10 The magnetic density vector distribution of molten aluminum on different planes in the NSC cell
(a) top surface, (b) bottom surface

The electromagnetic force distribution

The electromagnetic force distribution of molten aluminum along the horizontal direction is shown in Fig. 11. From Fig. 11(a), the electromagnetic force along the short axis x direction is dominant and the electromagnetic force along the long axis y direction is smaller. The reason is that level current of molten aluminum in the x direction and vertical current in the z direction are dominant. From Fig.11(b) for the NSC cell, we can see the electromagnetic forces in the x-axis and y axis have been significantly reduced because there is an opposing level electromagnetic force. The net effect reduces the fluctuation of molten aluminum in the NSC cell.

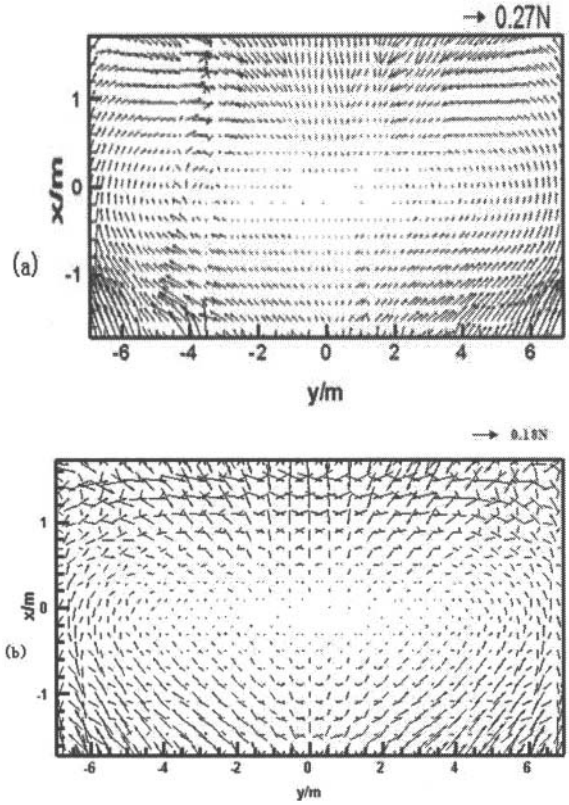

Fig. 11 The F_{xy} distribution at the bottom plane of molten aluminum in the traditional(a) and NSC(b) cell

Conclusions

(1)The voltage drop of the NSC is 0.066V lower than the traditional one, which means it is more energy efficient.

(2) The current density distribution in the NSC cathode is symmetric along the center line, there is a large level current at the short axis,

(3) Electromagnetic force in the NSC is smaller, since there is a force in the opposite direction which can reduce the electromagnetic force.

Acknowledgment

The project is supported by the National Natural Science Foundation of China (No.50934005) and National High Technology R & D program "863" project(2009AA063701).

Reference

[1] J. I. Buiza, "Electromagnetic Optimization of the V-350 Cell," *Light Metals,* (1989), 211-214.

[2] M. Dupuis and V. Bojarevics, "Weakly Coupled Thermo-electric and MHD Mathematical Models of an Aluminum Electrolysis Cell, *"Light Metals,* (2005), 449-454.

[3] V. Bojarevics and K. Pericleous, "Comparison of MHD Models for Aluminum Reduction Cells," *.Light Metals,* (2006), 347-352.

[4] G. V. Arkhipov and A. V. Rozin, "The Aluminum Reduction Cell Closed System of 3D Mathematical Models," *Light Metals,* (2005), 589-592.

[5] M. V. Romerio and M. A. Secretan, "Magne-tohydynamic equilibrium in aluminum electrolytic cells." *Computer Physics Reports,* (1986), 3: 327-360.June II .

[6] M. Dupuis, V. Bojarevics and D. Richard, "Impact of the Vertical Potshell Deformation on the MHD Cell Stability Behavior of a 500 kA Aluminum Electrolysis Cell," *Light Metals,* (2008), 409-412.

[7] Feng Naixiang, "New Cathodes in Aluminum Reduction Cells," *Light Metals 2010,* (2010), 405-408.